we expect the saturation power to be about $\rho P_{\rm beam}$, the total amplification factor will be about $N_{l_{\rm coh}}$, which is a large number whose typical magnitude is 10^5 to 10^7.

4.3.3 Temporal fluctuation and correlation of SASE

The SASE radiation consists of a random collection of a large number of coherent pulses, much like synchrotron radiation. To see this in the time domain, we construct the temporal amplitude by Fourier transforming the field in the frequency representation,

$$E_x(z,t) = \int d\nu\; E_\nu(z) e^{i\Delta\nu[(k_1+k_u)z-\omega_1 t]} e^{i(k_1 z-\omega_1 t)}, \tag{4.72}$$

with E_ν given by the growth SASE solution for the case of vanishing energy spread

$$E_\nu(z) = \frac{i\kappa_1 n_e}{2\rho k_u N_\lambda} \frac{e^{-i\mu 2\rho k_u z}}{\mu D'(\mu)} \sum_{j=1}^{N_e} e^{-i\nu\theta_j(0)}. \tag{4.73}$$

In general, the integral cannot be evaluated exactly due to the dependence of μ on $\Delta\nu$. However, in the limit that the energy spread is negligible, an approximate result can be obtained using the second order expansion derived in (4.66). Hence, we insert

$$\mu = -\frac{1}{2}\left[1 - \frac{\Delta\nu}{3\rho} + \frac{(\Delta\nu)^2}{36\rho^2}\right] + i\frac{\sqrt{3}}{2}\left[1 - \frac{(\Delta\nu)^2}{36\rho^2}\right] \tag{4.74}$$

into the exponential of μ, and the resulting expression is a Gaussian integral that can be done analytically. We obtain [6]

$$\begin{aligned} E_x(z,t) \propto \frac{e^{\sqrt{3}\rho k_u z}}{\sqrt{z}} \sum_{j=1}^{N_e} &\exp\left\{-i\omega_1\left[t - \frac{z}{c}(1+\rho\Delta\beta) - t_j\right]\right\} \\ &\times \exp\left\{-\frac{1+i/\sqrt{3}}{4\sigma_\tau^2}\left[t - \frac{z}{c}\left(1+\tfrac{2}{3}\Delta\beta\right) - t_j\right]^2\right\}, \end{aligned} \tag{4.75}$$

where the normalized difference of the average electron beam velocity from unity is $\Delta\beta \equiv 1 - \bar{\beta}_z = (1 + K^2/2)/2\gamma^2$, and the rms temporal width

$$\sigma_\tau = \frac{1}{\sqrt{3}\sigma_\omega} \approx \frac{1}{2\omega_1}\sqrt{\frac{z/\lambda_u}{\rho}}. \tag{4.76}$$

The total field profile (4.75) describes a sum of N_e wave packets of rms pulse length σ_τ that grow exponentially as they propagate. This random collection of modes has the essential properties of chaotic light, although in this case the power grows exponentially with z while its coherence length increases $\sim \sqrt{k_u z}$. Note that the relationship between the rms temporal and spectral widths of these modes differ from the usual $\sigma_\tau\sigma_\omega = 1/2$ due to the quadratic phase dependence in (4.75). We show an example of such temporal evolution of SASE in Fig. 4.5.

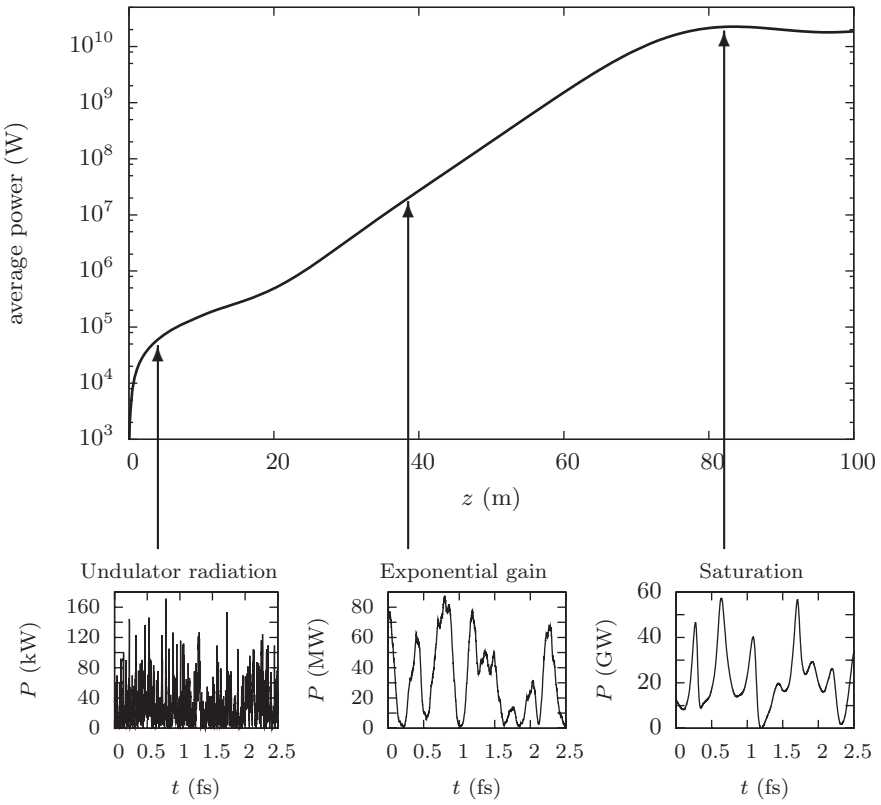

Figure 4.5 Evolution of the LCLS radiation power and temporal structure in a 1% time window. Courtesy of H.-D. Nuhn.

The wave packets are distributed randomly in time in a manner quite similar to undulator radiation. The phase velocity is less than the speed of light by the small factor $\rho\Delta\beta$, and it is interesting to note that the group velocity of each wave packet/temporal mode is [7]

$$v_g = \frac{c}{1 + 2\Delta\beta/3} \approx c\left(1 - \tfrac{2}{3}\Delta\beta\right). \tag{4.77}$$

The group velocity is slightly faster than the electrons (by $\Delta\beta/3$), but slower than c because the growing radiation mode is shaped by the FEL gain. Since the FEL gain is tied to the local electron bunching that moves with velocity $\bar{v}_z$, the gain tends to follow the electron beam; the interplay of radiation slippage and FEL gain leads to group velocity (4.77). Fig. 4.6 plots simulation results that confirm this interesting property in the exponential growth regime. Additionally, we see that the group velocity of these wave-packets is about equal to c after saturation, when the coupling between the radiation and the electron beam is greatly reduced.

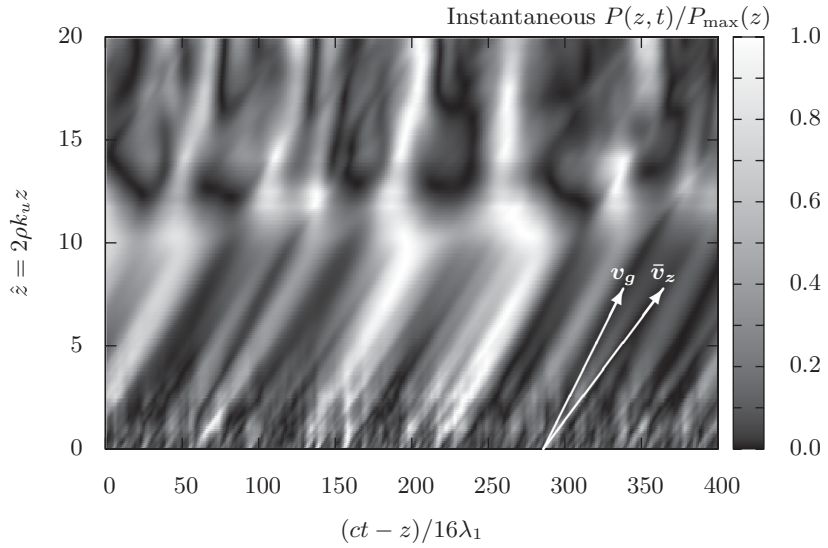

Figure 4.6 Simulation of the SASE radiation power as a function of the speed of light coordinate $ct - z$ and $\hat{z}$. The power at each location in z is scaled by the maximum at that location. Vertical lines correspond to wavefronts of electromagnetic waves in vacuum, while the arrows labeled $\bar{v}_z$ and v_g identify the slopes associated with the average electron beam speed along z and the theoretical SASE group velocity (4.77), respectively. The coherent regions move at the group velocity until saturation near $\hat{z} \sim 10$, after which the radiation becomes nearly uncoupled from the beam and moves approximately at the speed of light. Courtesy of W. Fawley.

As previously mentioned (and shown in Figs. 4.5-4.6), the temporal modes of SASE are randomly distributed over the pulse. This is because SASE is initialized by fluctuations in the beam current attributable to the discrete nature of the electron, namely, the shot noise. Thus, SASE is an example of a partially coherent wave, and its temporal fluctuations are those of chaotic light that we discussed in Sec. 1.2.5. Specifically, there are about $M \sim T/t_{\rm coh}$ temporal (and spectral) modes or spikes, and the integrated energy fluctuates by a relative amount $1/\sqrt{M}$ from shot-to-shot. A detailed description of SASE beyond these simple characteristics can be obtained using the techniques of statistical optics described in, e.g., [8]; such methods have been applied to SASE light in Refs. [9] and [10], among others. Here, we discuss a few such properties in a little more detail.

The characteristic time scale of the temporal fluctuations in SASE power is

given by the coherence length which we derived in (4.70):

$$t_{\rm coh} = \frac{\sqrt{\pi}}{\sigma_\omega} \;\to\; \frac{3}{\sqrt{2\pi z/L_{G0}}}\frac{\lambda_1}{c\rho} \sim \frac{\lambda_1}{c\rho}, \tag{4.78}$$

where the last two expressions have inserted the cold, 1D result and then assumed a propagation distance of order a few gain lengths. The field envelope in any given SASE pulse varies over times $\sim t_{\rm coh}$ as seen in Fig. 4.5, while the position and height of the intensity peaks are completely uncorrelated from pulse to pulse. These latter variations lead to shot-to-shot fluctuations in the SASE pulse energy which depend on both the coherence time and the temporal duration of the pulse T. To understand these fluctuations, we first consider a single SASE pulse. Using the fact that the electric field is approximately constant over the temporal duration $T \ll t_{\rm coh}$, it can be shown [11, 12] that the energy contained within a time interval much less than the coherence time is described by the negative exponential distribution, so that in this limit the probability $p(U)$ to measure the energy U over the time T is

$$T \ll t_{\rm coh}: \quad p(U) = \frac{1}{\langle U\rangle}\exp\!\left(-\frac{U}{\langle U\rangle}\right), \tag{4.79}$$

where $\langle U\rangle$ is the average energy contained in the time T. Equation (4.79) applies if $T \ll t_{\rm coh}$, for which the field will comprise one longitudinal mode, i.e., $M = 1$. On the other hand, in the limit $M \to \infty$ ($T \to \infty$), the energy will be normally distributed in accordance with the central limit theorem. A probability distribution that interpolates between these two limiting forms is the Gamma probability distribution; this line of reasoning underlies the suggestion in Ref. [9] that the statistics of the energy U in a flattop SASE pulse with duration T are governed by the Gamma distribution

$$p(U) = \frac{M^M}{\Gamma(M)}\frac{U^{M-1}}{\langle U\rangle^M}\exp\!\left(-M\frac{U}{\langle U\rangle}\right). \tag{4.80}$$

Here, $\langle U\rangle$ is the ensemble average of the electromagnetic energy for a SASE pulse of duration T, while $\Gamma(M)$ is the Gamma function. Using the properties of the Gamma distribution, M is related to the relative rms fluctuation in energy σ_U by [6, 9, 13]

$$M = \frac{1}{\sigma_U^2} = \frac{\langle U\rangle^2}{\langle U^2\rangle - \langle U\rangle^2} \approx \begin{cases} T/t_{\rm coh} & \text{if } T \gg t_{\rm coh} \\ 1 & \text{if } T \le t_{\rm coh} \end{cases}. \tag{4.81}$$

Thus, M characterizes the number of longitudinal degrees of freedom (or "modes") in the pulse, with (4.80)-(4.81) giving its more formal definition. Extensive simulations [9] have shown that (4.80) describes the energy probability distribution very well even up to saturation, while a more thorough statistical analysis has shown that the average number of intensity spikes in the time domain is about $0.7M$ [10].

For hard x-ray wavelengths, the coherence time determined by (4.78) is only

of order a few hundred attoseconds, while the SASE pulse duration T is dictated by the length of the electron beam. Typically, the electron beam is between ten and a few hundred femtoseconds in length, so that $M \gg 1$ and the Gamma distribution of shot-to-shot pulse energies approaches a Gaussian distribution with a small relative rms fluctuation given by $1/\sqrt{M}$. On the other hand, if the electron beam length is comparable to the coherence length so that $T \lesssim t_{\rm coh}$, than the resulting FEL radiation will be comprised of one longitudinally coherent mode at the expense of shot-to-shot stability: the energy variations from pulse to pulse will approach 100%.

The frequency domain exhibits very similar statistical properties. The full SASE bandwidth is about $2\sqrt{\pi}\sigma_\omega$, within which $\sim M$ independent spectral modes of width $2\pi/T$ are randomly distributed. At saturation where $z \sim \lambda_u/\rho$, the full bandwidth for a monoenergetic beam is $\sqrt{6\sqrt{3}}\rho\omega_1 \approx 3.2\rho\omega_1$. Additionally, it is interesting to consider the effect of a monochromator on the radiation statistics. To illustrate the basic physics, here we consider a single SASE pulse that initially comprises many longitudinal modes, so that $M \gg 1$ and $T \gg t_{\rm coh}$; more complete treatments can be found in Refs. [9, 10]. Passing the SASE pulse through a monochromator selects a certain frequency bandwidth in an analogous manner as the time interval T identifies a temporal region. If we denote the rms bandwidth of the monochromator by $\Delta\omega$, after the monochromator the average pulse energy $\langle U\rangle_{\Delta\omega} \approx (\Delta\omega/\sigma_\omega)\langle U\rangle$ if $\Delta\omega \lesssim \sigma_\omega$, and $\langle U\rangle$ otherwise. Assuming that the monochromator bandwidth is less than that of the SASE, $\Delta\omega \lesssim \sigma_\omega$, the monochromator reduces the spectral bandwidth and the number of spectral modes is given by

$$M_{\Delta\omega} \approx \begin{cases} \dfrac{\Delta\omega}{\sigma_\omega}\dfrac{T}{t_{\rm coh}} & \text{if } \Delta\omega \gg 1/t_{\rm coh} \\ 1 & \text{if } \Delta\omega \leq 1/t_{\rm coh} \end{cases}. \tag{4.82}$$

Thus, the radiation after the monochromator has a narrower bandwidth but larger energy fluctuations from pulse-to-pulse than the original SASE.

The statistical fluctuations discussed here can be generalized to three dimensions by redefining the total number of modes via $M = M_L M_T^2$, where M_L is the longitudinal mode number [whose limiting values are given by (4.81)], and M_T^2 are the number of transverse modes. Initially, the undulator radiation is also composed of many transverse modes $M_T^2 \gg 1$, so that in 3D the initial fluctuation level is relatively small. Since there is typically one transverse mode with the largest FEL gain, however, the exponential growth tends to preferentially select that single transverse mode, and $M_T \to 1$ after several gain lengths. Thus, the SASE fluctuations near saturation are largely governed by the 1D longitudinal statistics that we described above.